Article

# Contrasting forms of cocaine-evoked plasticity control components of relapse

PASCOLI, Vincent Jean, *et al*.

**Abstract**

Nucleus accumbens neurons serve to integrate information from cortical and limbic regions to direct behaviour. Addictive drugs are proposed to hijack this system, enabling drug-associated cues to trigger relapse to drug seeking. However, the connections affected and proof of causality remain to be established. Here we use a mouse model of delayed cue-associated cocaine seeking with ex vivo electrophysiology in optogenetically delineated circuits. We find that seeking correlates with rectifying AMPA (α-amino-3-hydroxy-5-methyl-4-isoxazole propionic acid) receptor transmission and a reduced AMPA/NMDA (N-methyl-D-aspartate) ratio at medial prefrontal cortex (mPFC) to nucleus accumbens shell D1-receptor medium-sized spiny neurons (D1R-MSNs). In contrast, the AMPA/NMDA ratio increases at ventral hippocampus to D1R-MSNs. Optogenetic reversal of cocaine-evoked plasticity at both inputs abolishes seeking, whereas selective reversal at mPFC or ventral hippocampus synapses impairs response discrimination or reduces response vigour during seeking, respectively. Taken together, we describe how information integration in the nucleus [...]

Reference

PASCOLI, Vincent Jean, *et al*. Contrasting forms of cocaine-evoked plasticity control components of relapse. *Nature*, 2014, vol. 509, no. 7501, p. 459-64

PMID : 24848058
DOI : 10.1038/nature13257

# Contrasting forms of cocaine-evoked plasticity control components of relapse

Vincent Pascoli[1]*, Jean Terrier[1]*, Julie Espallergues[3-5], Emmanuel Valjent[3-5], Eoin Cornelius O'Connor[1] and Christian Lüscher[1, 2]

* These authors contributed equally to this work

**Affiliations:**

[1] Dept. of Basic Neurosciences, Medical Faculty, University of Geneva, CH-1211 Geneva, Switzerland.
[2] Clinic of Neurology, Dept. of Clinical Neurosciences, Geneva University Hospital, CH-1211 Geneva, Switzerland.
[3] INSERM, U661, Montpellier, F-34094, France.
[4] CNRS, UMR-5203, Institut de Génomique Fonctionnelle, Montpellier, F-34094, France.
[5] Universités de Montpellier 1 & 2, UMR-5203, Montpellier, F-34094, France.

To whom correspondence should be addressed. E-mail: christian.luscher@unige.ch

**Summary**

Nucleus accumbens (NAc) neurons serve to integrate information from cortical and limbic regions to direct behavior. Addictive drugs are proposed to hijack this system, enabling drug associated cues to trigger relapse to drug seeking. However, the connections affected and proof of causality remain to be established. Here we use a mouse model of delayed cue-associated cocaine seeking with *ex vivo* electrophysiology in optogenetically delineated circuits and find that seeking correlates with rectifying AMPAR transmission and a reduced AMPA/NMDA ratio at mPFC to NAc shell D1R-MSNs. In contrast, the AMPA/NMDA ratio is increased at vHipp to D1R-MSN synapses. Optogenetic reversal of cocaine-evoked plasticity at both inputs abolished seeking, while selective reversal at mPFC or vHipp synapses impaired response discrimination or reduced response vigor during seeking, respectively. Taken together, we describe how information integration in the NAc is commandeered by cocaine at discrete synapses to permit relapse. Our approach holds promise for identifying synaptic causalities in other behavioral disorders.

## INTRODUCTION

The nucleus accumbens (NAc) is a point of convergence for excitatory afferents arising from limbic and cortical regions, including the basolateral amygdala (BLA), ventral hippocampus (vHipp) and the medial prefrontal cortex (mPFC). From pharmacology, lesion and imaging experiments, each of these regions is thought to signal distinct information to the NAc during reward-related situations. Specifically, the BLA signals emotional valence, the vHipp provides contextual relevance, while the mPFC provides action-outcome information
(Berridge and Kringelbach, 2013; Robbins and Everitt, 1996). NAc neurons select and integrate information from these diffuse regions and signal to the basal ganglia motor system to guide appropriate behaviors, like foraging in response to feeding relevant signals(Humphries and Prescott, 2010; Papp et al., 2011). This neural circuitry is also involved in core features of drug addiction, such as craving and relapse in response to drug associated cues after withdrawal periods(Everitt and Robbins, 2005; Kalivas and Volkow, 2005). Understanding how this circuitry is "hijacked" following drug experience and how drug-evoked alterations are causally related to drug-adaptive behaviors, like relapse, is fundamental to define the pathophysiology of addiction.

The task of information processing and output in the NAc falls to medium-sized spiny neurons (MSNs), representing 95 % of NAc neurons and broadly divisible into two equally sized classes according to the dopamine receptors expressed(Valjent, 2013). Both NAc D1 receptor (D1R)-MSN and D2 receptor (D2R)-MSN subtypes receive excitatory afferents from the BLA, vHipp and mPFC
(MacAskill et al., 2012; Papp et al., 2011), but differ in their projection targets(Humphries and Prescott, 2010; R. J. Smith et al., 2013). Owing to the arrangement of synapses on MSN

spines, excitatory transmission arriving onto the spine head is subject to strong modulation by dopamine from the ventral tegmental area (VTA) arriving at the spine neck(Freund et al., 1984). Indeed, dopamine gates excitatory transmission, allowing synaptic adaptations and modulation of reward-related behaviors
(Cerovic et al., 2013; Goto and Grace, 2008; Saddoris et al., 2013). Accumbal dopamine transients induced by addictive drugs are likely key for inducing circuit adaptations that divert behavior towards compulsive drug seeking and heighten the risk for relapse after prolonged withdrawal (DiChiara and Bassareo, 2007; Schultz, 2011). Relapse is associated with exposure to drug cues, it is context dependent and requires knowledge of what actions result in drug delivery(Everitt and Robbins, 2005). Therefore, this behavior is likely underpinned by a memory trace, formed within the reward circuitry during drug use
(Hyman, 2005; Lüscher and Malenka, 2011). However, the nature of this trace and the causal implications remain elusive.

Much literature has described induction requirements and expression mechanisms for drug-evoked plasticity at excitatory synapses, including those of the NAc (Lüscher and Malenka, 2011). The time after the last drug exposure is important, as the expression of some forms of plasticity can take days or weeks(Kourrich et al., 2007; Ortinski et al., 2012). Therefore, establishing a causal link between drug-evoked plasticity and drug-adaptive behaviors has been difficult. Pharmacological manipulation of AMPA receptors implicates NAc glutamatergic transmission in cue-associated cocaine seeking(Conrad et al., 2008; Cornish and Kalivas, 2000), but many questions remain. Do different excitatory inputs change in the same way onto D1R- and D2R-MSNs following withdrawal from cocaine self-administration? Could drug-evoked alterations at specific inputs be causally linked to specific components of drug-adaptive behaviors, like relapse? Here we utilise cell-type

specific reporter lines and optogenetics to address these questions, taking an approach that may also be applied in other behavioral disorders to establish synaptic causalities (Extended Data Fig. 1).

## METHODS

### Animals

Mice were C57BL/6 or heterozygous BAC transgenic mice in which tomato expression was driven by dopamine D1 receptor (D1R) (Drd1a-tdTomato from Jackson Laboratories) gene regulatory elements or eGFP driven by dopamine D2 receptor (D2R) (Drd2-eGFP from GENSAT) gene regulatory elements. Both males and females were used. Transgenic mice had been backcrossed in the C57BL/6 line for a minimum of four generations. Mice were single housed after surgery. All animals were kept in a temperature- and humidity-controlled environment with a 12 h light/12 h dark cycle (Lights on at 7:00 am). All procedures were approved by the Institutional Animal Care and Use Committee of the University of Geneva.

### Stereotaxic injections

AAV1-CAG-ChR2-eYFP (eYFP; also called venus) or AAV1-CAG-eYFP (for control mice) produced at the University of North Carolina (Vector Core Facility) was injected into the medial prefrontal cortex (mPFC; focusing on the infralimbic area), ventral subiculum of the hippocampus (vHipp) or basolateral amygdala (BLA) of 5 to 6 week old mice. Anesthesia was induced at 5% and maintained at 2.5% isoflurane (w/v) (Baxter AG) during the surgery. The animal was placed in a stereotaxic frame (Angle One) and craniotomies were performed using stereotaxic coordinates adapted from a mouse brain atlas (Franklin and Paxinos, 2008) (for mPFC: anterior-posterior (AP) = +1.9; medial-lateral (ML) = ±0.3; dorsal-ventral (DV, from the surface of the brain) = -2.5; for vHipp : AP = -3.5; ML = ±2.8; DV = -4.2; for BLA : AP = –1.4; ML = ±3.0; DV = –3.8). Injections of virus (0.5 µl per injection site) were carried out using graduated pipettes (Drummond Scientific Company), broken back to a tip diameter of 10–15 µm, at an infusion rate of ~0.05 µl $min^{-1}$. Injections of ChR2 were made a minimum of one week prior to the self-administration surgery, and thus optogenetic manipulations typically occurred no sooner than 7 weeks after the injection. For anterograde tracing studies**,** 6-8 week old C57BL/6J mice were infected

with both AAV5-EF1α-mCherry in the mPFC and AAV5-EF1α-eYFP in the vHipp to allow observation of multiple inputs into nucleus accumbens (NAc).

For retrograde tract-tracing studies**,** mice were stereotaxically injected with the retrograde tracer, cholera toxin subunit B conjugated to a fluorescent marker (CTB, Alexa Fluor 594 conjugate, Molecular Probes, Leiden, The Netherlands). Microinjection needles were placed into the NAc medio-dorsal (AP = +1.18; ML = +0.5; DV = -3.7) or NAc ventral medio-ventral (AP = +1.18; ML = +0.5; DV = -4.2) and 0.5 µl was injected over 5 min. The injector was left in place for an additional 5 min to allow for diffusion of CTB particles away from the injection site. Animals returned to their home cages for 14 days prior to tissue preparation.

**Tissue preparation and immunofluorescence**

Mice were rapidly anaesthetized with pentobarbital (500 mg/kg, i.p., Sanofi-Aventis, France) and transcardially perfused with 4% (weight/vol.) paraformaldehyde in 0.1 M sodium phosphate buffer (pH 7.5) (Bertran-Gonzalez et al., 2008)). Brains were post-fixed overnight in the same solution and stored at 4°C. Thirty-□m thick sections were cut with a vibratome (Leica, France) and stored at -20°C in a solution containing 30% (vol/vol) ethylene glycol, 30% (vol/vol) glycerol, and 0.1 M sodium phosphate buffer, until they were processed for immunofluorescence. Sections were processed as follows: free-floating sections were rinsed in Tris-buffered saline (TBS: 0.25 M Tris and 0.5 M NaCl, pH 7.5), incubated for 5 min in TBS containing 3% $H_2O_2$ and 10% methanol (vol/vol), and then rinsed three times 10 min in TBS. After 15 min incubation in 0.2% (vol/vol) Triton X-100 in TBS, sections were rinsed three times in TBS again. Sections were then incubated for 1 h in a solution of BSA 3% in TBS. Finally, they were incubated 72 h at 4°C with the primary antibodies mouse anti-DARPP-32 (1:1000 gift from P. Greengard, mouse monoclonal clone C54 (Ouimet et al., 1984)) and rabbit anti-RFP (1:1000, Medical & Biological Laboratories, rabbit polyclonal, lot #042). After incubation with the primary antibodies, sections were rinsed three times for 10 min in TBS and incubated for 45 minutes with goat Cy3- and Cy5-coupled secondary antibodies (1:400, Jackson Labs, lot #114787 and Life techonologies #1305923). Sections were rinsed for 10 min twice in TBS and twice in TB (0.25 M Tris) before mounting in 1,4-diazabicyclo-[2.2.2]-octane (DABCO, Sigma-Aldrich). Double- or triple-labeled images from each region of interest were obtained using sequential laser scanning confocal microscopy (Zeiss LSM510 META). Photomicrographs were obtained

with the following band-pass and long-pass filter settings: GFP (band pass filter: 505-530), Cy3 (band pass filter: 560-615) and Cy5 (long-pass filter 650). The objectives and the pinhole setting (1 airy unit) remained unchanged during the acquisition of a series for all images. The thickness of the optical section is ~1.6 µm with a 20X objective and ~6 µm with a 10X objective. GFP labeled neurons were pseudo-colored green and other markers immunoreactive neurons were pseudo-colored red or blue. For images showing infected structure with AAV1-CAG-ChR2-eYFP, 30-µm thick coronal sections were cut with a vibratome (Leica, France), stained with Hoechst (Sigma-Aldrich) and mounted with Mowiol (Sigma-Aldrich). Full images of brain slices from mPFC, BLA and vHipp were obtained with a MIRAX (Carl Zeiss) system equipped with a Plan-Apochromat 20x/0.8 objective, together with DAPI (emission: 455/50) and FITC (emission: 515-565) filters.

**Implantation of jugular vein catheter**

The surgical procedure was adapted from (Thomsen and Caine, 2006; Chistyakov and Tsibulsky, 2006). Mice were anesthetized with a mix of ketamine (60 mg/kg, Ketalar®) and Xylazine (12 mg/kg, Rompun®) solution. Catheters (CamCaths, model MIVSA) made of silicone elastomer tubing (outside diameter 0.63 mm, inside diameter 0.30 mm) were inserted 1.0-1.2 cm in the right jugular vein, about 5 mm from the pectoral muscle, in order to reach the right atrium. The other extremity of the catheter was placed subcutaneously in the mid-scapular region and connected to stainless steel tubing appearing outside of the skin. Blood reflux in the tubing was checked to confirm correct placement of the catheter. Mice were allowed to recover for 3 to 5 days before the start of drug self-administration training and received antibiotics (Baytril® 10%, 1 ml in 250 ml of water) in the drinking water during this period. Catheters were flushed daily with a heparin solution (Heparin "Bichsel" ®) in saline (30 IU) during the recovery period and just before and after each self-administration session.

**Self-administration apparatus**

All behavioral experiments were performed during the light phase and took place in mouse operant chambers (ENV-307A-CT, Med Associates Inc.) situated in sound-attenuating cubicle (Med Associates Inc.). Two retractable levers were present on both sides of one wall of the chamber and a food pellet dispenser was also present only for procedures involving food delivery. A cue-light was located above each lever and a house light was present in each chamber. During intravenous drug self-administration sessions, the stainless steel

tubing of the catheter device was connected through a CoEx™ PE/PVC tubing (BCOEX-T25, Instech Solomon) to a swivel (Instech Solomon) and then an infusion pump (PHM-100, Med-Associates). The apparatus was controlled and data captured using a PC running MED-PC IV (Med-Associated).

**Drug self-administration acquisition**

Mice were deprived of food for 12 hours before the first self-administration session in order to promote exploratory activity. No food shaping was undertaken and mice were given food access *ad libitum* after the first session. Each session was 120 minutes in duration and started with the illumination of the house light and the insertion of the two levers into the operant chamber. During the first five sessions, a single press on the active lever (termed fixed-ratio 1, or FR1) resulted in an infusion of 0.75 mg/kg of cocaine (cocaine hydrochloride, provided by the pharmacy of Geneva University Hospital, dissolved in 0.9% saline at 0.75 mg/mL and delivered at 0.0177 mL/sec as a unit dose depending on the mouse weight) paired with a 5-s continuous illumination of the cue light above the active lever. Completion of the fixed-ratio also initiated a timeout period of 20 seconds during which cocaine was no longer available. For the next five sessions two lever presses were needed to activate the infusion pump (FR2). The active lever (left or right lever) was randomly assigned for each mouse. In order to avoid an overdose of cocaine, a maximum of 45 infusions were allowed per session. Only mice having reached a stable rate of at least 70 % of correct lever responses (number of active lever responses divided by total lever responses over the 3 last session of acquisition) were included in the study. Saline control mice undertook the same procedure as cocaine mice except that saline (NaCl 0.9 % B Braun®) replaced cocaine infusions. After acquisition, mice were randomly attributed to either behavior or electrophysiology experiments (except wild-type mice which were only used in behavior experiments). Recordings were never performed after cue-associated seeking tests in order to avoid confounding effects on synaptic transmission (Gipson et al., 2013).

**Optic fiber cannulation and *in vivo* optogenetic stimulation protocols**

After completing the acquisition of self-administration, all mice were put in forced abstinence for 30 days in their home cage. At days 15-20, mice destined for seeking tests or *ex vivo* validation were bilaterally implanted with chronically indwelling optic fiber cannula (made in house as described in (Sparta et al., 2011)) into the NAc (AP = +1.5; ML = ±1.6; DV = -3.9 with a 10° angle) using stereotaxic apparatus as described above. Two screws

were fixed into the skull to support the implant, which was further secured with dental cement.

DPSS blue light lasers (MBL-473/50 mW; CNI lasers, Changchun, China) connected to the indwelling fiber optic via customized patch cords (BFL37-200 Custom; Thor Labs, Dachau, Germany) and a double rotary joint (FRJ-1X2i; Doric Lenses, Quebec, Canada) allowed mice to move freely during stimulation. The laser was triggered to deliver 4 ms pulses at 1 Hz or 13 Hz for 10 min, and the protocol was applied in the home cage 4 hours before the first drug-seeking session or sacrificing for *ex-vivo* electrophysiology recordings. Mice from the control group were, in a randomized manner, either not infected with ChR2 or infected with eYFP only and received one of the optogenetic protocols, or were infected with ChR2 but were not exposed to light-stimulation. Seeking behavior did not differ amongst these three control conditions, so the data were collapsed.

**Test of cue-associated drug seeking**

Thirty days after the final self-administration session (i.e. day 40), mice were assigned to optogenetic protocol groups (Ctrl, 1 or 13 Hz) according to performance during SA acquisition, such that acquisition did not differ between the groups. Control animals were included for each batch of tested animals explaining the greater number of mice in the control group. The cue-associated drug seeking test was a 60 minute session, identical to the cocaine acquisition period (house light on, insertion of the two levers), except that one press on the active lever (FR1 schedule) now triggered illumination of the cue light for 5 seconds but without a cocaine infusion or a timeout period. The infusion pump was also activated during the drug-seeking session, since the pump noise provided an additional drug associated cue. One week later (i.e. day 48), mice undertook a second drug seeking session (with no further optogenetic stimulation 4 hours before) to assess the persistence of the optogenetic protocol on seeking behavior. At the end of any behavioral experiment, mice were euthanized and brains fixed in PFA to prepare histological slices for verification of ChR2 expression and cannula placement (see Extended Data Fig. 9)

**Food training after drug seeking**

Immediately following the second drug-seeking test, subgroups of mice were food deprived for 12 hours and then started 9 consecutive sessions of operant training for food to examine whether optogenetic protocols had long-term effects on the acquisition of new learning for a

natural reward. The test was performed in similar chambers as used previously (ENV-307A-CT, Med Associates Inc.), except that two nose-poke holes were present instead of levers at each side of a food pellet dispenser. One nose-poke in the active hole (randomly assigned) illuminated the cue light for five seconds and triggered the delivery of one food pellet (50 % sucrose, AIN-76A Rodent tablet 20 mg, Testdiet®). The response requirement was set at FR1 for sessions 1-3, FR2 for sessions 4-6 and FR3 for sessions 7-9. The house light was turned off during the entire session. Each session ended after 30 minutes or when 45 pellets had been delivered, whichever occurred first. Each mouse received 2.7-3 g/day of standard lab chow during the food training procedure in order to maintain a stable body weight without any further weight gain.

**Effect of optogenetic protocols on cue-associated food seeking**

To assess the specificity of the optogenetic treatment for drug vs. food cue-associated seeking, we also tested a new cohort of mice for cue-associated food seeking after the optogenetic protocol. Mice underwent food training in the exact same conditions as for the cocaine self-administration group except that cocaine infusions were replaced by sucrose pellet delivery. Sessions ended after 30 minutes or when 45 pellets were delivered, whichever occurred first. After implantation of fiber optic cannula at day 15-20 of forced abstinence from sucrose pellet consumption, mice were assigned to the control or 13 Hz groups (such that acquisition did not differ between the groups) and received the optogenetic treatment 4 h before a test for food-reward seeking that was undertaken in the same way as the test for cocaine seeking. The sound of the pellet dispenser was also paired with the food cue light during the session. Food seeking sessions lasted 30 minutes. Mice received 2.7-3g/day of standard lab chow over the entire procedure in order to maintain a stable body weight (no weight gain).

**Slice electrophysiology**

Coronal 200–250 μm slices of mouse brain were prepared in cooled artificial cerebrospinal fluid (ACSF) containing (in mM): NaCl 119, KCl 2.5, MgCl 1.3, $CaCl_2$ 2.5, $Na_2HPO_4$ 1.0, $NaHCO_3$ 26.2 and glucose 11, bubbled with 95% $O_2$ and 5% $CO_2$. Slices were kept at 32–34 °C in a recording chamber superfused with 2.5 ml $min^{-1}$ ACSF. Visualized whole-cell voltage-clamp recording techniques were used to measure holding and synaptic responses of medium spiny neurons (MSNs) of the nucleus accumbens shell, identified by the presence of the eGFP or td-Tomato of BAC transgenic mice by using a fluorescent microscope

(Olympus BX50WI, fluorescent light U-RFL-T). Note that when using ChR2-eYPP in BAC transgenic mice, D2R-MSNs were identified as D2R-eGFP positive neurons in Drd2-eGFP mice, which were possible to visualise against fluorescence from ChR2-eYFP, or as tomato negative neurons in Drd1a-tdTomato mice. D1R-MSNs were always identified as tomato positive cells. This approach was validated in a previous report (Pascoli et al 2011). The holding potential was −70 mV, and the access resistance was monitored by a hyperpolarizing step of −14 mV with each sweep, every 10 s. The liquid junction potential was small (−3 mV), and therefore traces were not corrected. Experiments were discarded if the access resistance varied by more than 20%. Currents were amplified (Multiclamp 700B, Axon Instruments), filtered at 5 kHz and digitized at 20 kHz (National Instruments Board PCI-MIO-16E4, Igor, WaveMetrics). All experiments were carried out in the presence of picrotoxin (100 μM).

For recordings of light- and electrically-evoked EPSCs the internal solution contained (in mM) 130 CsCl, 4 NaCl, 5 creatine phosphate, 2 $MgCl_2$, 2 $NA_2ATP$, 0.6 $NA_3GTP$, 1.1 EGTA, 5 Hepes, 0.1 mM spermine. In some cases, QX-314 (5 mM) was added to the solution to prevent action currents. Synaptic currents were electrically evoked by stimuli (50–100 μs) at 0.1 Hz through bipolar stainless steel electrode placed onto the tissue. For optogenetic experiments, light-EPSCs were evoked with 4 ms blue light pulses from an optic fiber directed at the NAc shell that was coupled to a DPSS blue light laser. Low-frequency stimulation (LFS; 1 or 13 Hz for 10 min) was applied with 4 ms light pulses and the magnitude of LTD was determined by comparing average EPSCs that were recorded 20–30 min after induction to EPSCs recorded immediately before induction. To isolate AMPAR-evoked EPSCs the NMDA antagonist (D)-2-amino-5-phospho- novaleric acid (D-AP5, 50 μM) was bath applied. The NMDAR component was calculated as the difference between the EPSCs measured in the absence and in the presence of D-AP5. The AMPAR/NMDAR ratio was calculated by dividing the peak amplitudes. The rectification index (RI) of AMPAR was calculated as the ratio of the chord conductance calculated at negative potential divided by chord conductance at positive potential. Note that in example traces, stimulation artifacts were removed.

For recordings of mEPSCs the internal solution contained (in mM): 140 K Glu, 2 $MgCl_2$, 5 KCl, 0.2 EGTA, 10 Hepes, 4 $NA_2ATP$, 0.3 $Na_3GTP$, 10 creatine phosphate. Miniature

EPSCs were recorded in the presence of tetrodotoxin (0.5 μM). The frequency, amplitudes and kinetic properties of these currents were then analysed using the Mini Analysis software package (v.4.3, Synaptosoft). Note that recordings were performed with the electrophysiologist blinded to the SA condition (cocaine or saline), although for practical reasons the experimenter was aware of other conditions (e.g. ChR2 infected or not e.t.c.).

**Statistics**

No statistics were used to determine group sample size, however sample sizes were similar to those used in previous publications from our group and others reporting self-administration in mice. Multiple comparisons were first subject to mixed-factor analysis of variance (ANOVA) defining both between (e.g. D1R- or D2R-MSN *cell*; saline or cocaine SA *groups*; control, 1 Hz or 13 Hz *protocols*; BLA, vHIPP, mPFC *inputs* etc) and/or within (e.g. active or inactive *levers*) group factors. Where significant main effects or interaction terms were found ($P \leq 0.05$; or $P \leq 0.1$ indicative of a trend), further comparisons were made by two-tailed *t*-test with Bonferroni corrections applied when appropriate (i.e. the level of significance equals 0.05 divided by the number of comparisons). Single comparisons of between or within group measures were made by two-tailed non-paired or paired student *t*-test, respectively. ANOVAs for main figures are provided (see Extended Data Tables 1a-b)

**RESULTS**

**Cocaine-evoked plasticity at D1R-MSNs**

To characterize drug-evoked plasticity in identified NAc MSNs at a time point when relapse can be observed, BAC transgenic mice expressing fluorescent proteins under the control of the D1R or D2R promoter were first trained to self-administer intra-venous (i.v.) cocaine(Ambroggi et al., 2009). Control mice that received only i.v. saline infusions quickly stopped responding, while cocaine self-administration (SA) mice learned to discriminate between the active and inactive levers and responded almost exclusively on the active lever at the end of the acquisition phase, confirming successful acquisition of cocaine SA (Fig. 1a-b).

Thirty days after the last SA session, whole-cell recordings were made *ex vivo* in identified NAc MSNs with excitatory postsynaptic currents (EPSCs) elicited by electrical stimulation to obtain a global overview of cocaine-evoked plasticity (Fig. 1c). The rectification index (RI) of AMPAR-EPSCs was increased selectively in D1R-MSNs from cocaine-SA mice, suggesting the presence of GluA2-lacking calcium-permeable AMPARs (CP-AMPARs;(Liu and Zukin, 2007)). The ratio of the amplitude of AMPAR- and NMDAR-EPSCs (A/N ratio) recorded in the same cells, which provides a measure of synaptic strength, was also increased only in D1R-MSNs from cocaine SA mice (Fig. 1c). At first glance, it was surprising to observe these two forms of plasticity in the same neuron, since CP-AMPARs exhibit reduced conductance at +40 mV that would produce a decreased A/N ratio, if NMDA were unchanged. One potential explanation is that cocaine induced several contrasting forms of plasticity that segregate between different inputs onto the same D1R-MSNs. In support of this idea, a recent study reported an increased A/N ratio specifically at vHipp to NAc synapses following chronic non-contingent cocaine injections, without however resolving the MSN identity(Britt et al., 2012).

**Cocaine-evoked plasticity at identified inputs**

To explore the possibility that distinct afferents to the NAc undergo contrasting forms of plasticity following cocaine SA, the optogenetic effector channelrhodopsin tagged with eYFP (ChR2-eYFP) was virally expressed by stereotaxic injection into the BLA, vHipp or mPFC of BAC transgenic reporter mice (Fig. 2a). Retrograde labelling with cholera toxin subunit B (CTB) in the dorso- or ventro-medial NAc shell confirmed these regions as providing major afferents (Extended Data Fig. 2a), while anterograde labelling of different inputs with distinct fluorescent markers identified the juxtaposition of fibers in the NAc

(Extended Data Fig. 3), in agreement with studies reporting the convergence of inputs onto the same MSN(French and Totterdell, 2003; 2002; Goto and Grace, 2005). Whole-cell recordings from mice infected with ChR2-eYFP in each region confirmed that inputs were excitatory (Extended Data Fig. 2c). Input and cell-type specific plasticity was then evaluated *ex vivo* in the NAc shell from cocaine or saline SA mice following one month of withdrawal.

Recordings of light-evoked AMPAR-EPSCs first confirmed that the strongest input onto the NAc arises from the hippocampus(Britt et al., 2012) and that cocaine SA evoked a significant potentiation of AMPAR-EPSC amplitudes only at vHipp and mPFC inputs onto D1R-MSNs (Fig. 2b). No change was observed at any input onto D2R-MSNs (Extended Data Fig 4a). Remarkably, rectification of the I/V curve was detected only at mPFC to D1R-MSN synapses in cocaine SA mice, but not at vHipp or BLA to NAc synapses (Figure 2c). Thus, cocaine SA triggered the insertion of CP-AMPARs only at mPFC to D1R-MSNs synapses. Confirming findings with electrical stimulation, I/V curves were linear for all inputs onto D2R-MSNs in cocaine SA mice (Extended Data Fig. 4b). Regarding the A/N ratio, in cocaine SA mice it was decreased at mPFC to D1R-MSN synapses (consistent with the poor conductance of CP-AMPARs at +40 mV), but increased at vHipp to D1R-MSN synapses and unaffected at BLA synapses (Fig. 2d). Cocaine SA evoked no change in the A/N ratio at any input onto D2R-MSNs (Extended Data Fig. 4c). Note that in baseline conditions (i.e. saline SA mice) both RI and AMPAR/NMDA ratios were similar across all inputs onto D1R- and D2R-MSNs, as predicted from electrical recordings. Collectively, these results demonstrate that cocaine SA and withdrawal results in contrasting forms of plasticity at specific inputs onto the same accumbal D1R-MSN.

**Homosynaptic effects of optogenetic protocols**

Having identified specific inputs onto NAc shell D1R-MSNs that express drug-evoked plasticity, we wanted to test for a causal link to cue-associated drug seeking. To this end, we aimed to develop optogenetic protocols *ex vivo* that could restore basal synaptic transmission (Fig. 3a,f). But more than a complete erasure of cocaine-evoked plasticity, we sought to parse the relationship between plasticity at identified synapses to cue-associated seeking behavior.

Since synapses were essentially potentiated following cocaine SA, optogenetic protocols were employed that could trigger long-term depression (LTD). When recording light-evoked AMPAR-EPSCs selectively at vHipp to D1R-MSNs, application of a 1 Hz NMDAR-dependent LTD protocol(pascoli et al., 2011) significantly depressed EPSCs in both saline and cocaine SA groups (Fig. 3b). At the same input, a 13 Hz extrasynaptic metabotropic glutamate receptor (mGluR) dependent LTD protocol (Extended Data Fig. 5a;(Robbe et al., 2002)) triggered a depression in the cocaine SA group that was significantly attenuated when compared to controls (Fig. 3c). The consequence of applying either protocol on cocaine-evoked plasticity at vHipp to NAc synapses (i.e. homosynaptic effects) was then examined. As described above, CP-AMPARs were not present at vHipp to NAc synapses after cocaine SA and neither the 1 nor 13 Hz vHipp protocol further altered the linear IV curve or RI at this input. Remarkably however, the 1 Hz, but not the 13 Hz vHipp protocol normalized the cocaine-evoked increase in the A/N ratio at this input (Fig. 3d-e). Note that in the saline SA group, the 1 or 13 Hz vHipp protocols had little impact on the A/N ratio at these synapses, which was already low at baseline (Fig. 3b-e).

These experiments were repeated, but now isolating mPFC to D1R-MSN synapses (Fig. 3f). The 1 Hz mPFC protocol only slightly depressed AMPAR-EPSCs in the cocaine SA group, while the depression was significantly larger in controls (Fig. 3g). This finding concurs with a previous study where NMDAR-dependent LTD was altered in "cocaine-addicted" rats(Kasanetz et al., 2010). The 13 Hz mPFC protocol was actually more efficient in the cocaine SA group (Fig. 3h), which is of particular interest because mGluR activation can remove CP-AMPARs at many synapses throughout the brain
(Clem and Huganir, 2010; Lüscher and Huber, 2010; Mccutcheon et al., 2011). Both protocols triggered comparable LTD of AMPAR-EPSCs in D2R-MSNs from saline and cocaine SA mice (Extended Data Fig. 5b). The homosynaptic effects of these protocols on cocaine-evoked plasticity at mPFC to NAc synapses was then examined which, as described above, indicated the presence of CP-AMPARs. Consistent with LTD experiments, the 13 Hz, but not the 1 Hz mPFC protocol normalized both the rectifying I/V curve and the depressed A/N ratio (Fig. 3i-j), pointing to removal of CP-AMPARs from mPFC to D1R-MSN synapses. In the saline SA group the 1 Hz, but not the 13 Hz mPFC protocol significantly reduced the A/N ratio, while the RI remained unchanged in either case.

**Heterosynaptic effects of optogenetic protocols**

After evaluating the 1 and 13 Hz protocols on light-evoked homosynaptic transmission, the possibility of heterosynaptic effects was explored *ex vivo* (i.e. normalization of cocaine-evoked plasticity at an input other than which the protocol was applied). Indeed, *in vivo* recordings have demonstrated that activation of one excitatory NAc input can trigger heterosynaptic plasticity(Goto and Grace, 2005).

Optogenetic LTD protocols were applied onto slices at vHipp or mPFC to NAc inputs but EPSCs were evoked with electrical stimulation, thus recruiting transmission from multiple afferents (Fig. 4a). The cocaine-evoked rectification of AMPAR transmission was restored by the 13 Hz protocol whether applied at vHipp or mPFC to NAc synapses (Fig. 4b). Since rectification was only found at mPFC to D1R-MSN synapses, the 13 Hz vHipp protocol must have triggered normalization of this synapse heterosynaptically, most likely by activating mGluRs at neighbouring synapses through glutamate spillover or intracellular signalling. With respect to the A/N ratio, which was increased in the cocaine SA group when recorded with electrical stimulation, normalization was observed using the 1 Hz vHipp protocol (Fig. 4c). This likely reflected a homosynaptic effect as reported above (see Figure 3e). However, the 13 Hz mPFC protocol, in addition to removing rectifying AMPARs, also restored the A/N ratio; a heterosynaptic effect likely occurring through glutamate spillover activating NMDARs at vHipp to D1R-MSN synapses. Note that the 13 Hz vHipp protocol, in contrast to its heterosynaptic effect on RI, did not elicit a homosynaptic reduction in the A/N ratio, possibly because NMDAR activation was too strong to elicit depression(Bienenstock et al., 1982; Lüscher and Malenka, 2012). Since our initial validations were performed *ex vivo*, we also confirmed that optogenetic protocols were efficient in normalizing cocaine-evoked plasticity when applied *in vivo* (Extended Data Fig. 6 and 7, which includes additional discussion). Taken together, this approach led to an advantageous scenario to test the causality of contrasting forms of drug-evoked plasticity in cue-associated cocaine seeking, since plasticity at mPFC or vHipp to D1R-MSNs could be restored separately using the using the 13 Hz vHipp or the 1 Hz vHipp protocol, respectively, or together by using the 13 Hz mPFC protocol.

**Causal link to components of cocaine seeking**

Now we applied optogenetic protocols in SA mice to directly test causality between drug-evoked plasticity at identified inputs and a drug-adaptive behavior relevant to addiction. Following one month of withdrawal from SA, mice underwent a cue-associated seeking test, a rodent model of relapse, with optogenetic protocols applied once, 4 hours before the test (Fig. 5a, b).

The 1 Hz vHipp protocol (i.e. reversing cocaine-evoked plasticity only at vHipp to D1R MSNs) significantly reduced cue-associated lever pressing, a measure of response vigor, although cocaine seeking *per se* was still present. The 13 Hz vHipp protocol (i.e. inducing a heterosynaptic reversal of plasticity at mPFC to D1R-MSNs) led to increased inactive lever responding, pointing to impaired action-outcome response discrimination. The 1 Hz mPFC protocol (i.e. no effect on cocaine-evoked plasticity) was without effect on seeking behavior. Finally, the 13 Hz mPFC protocol (i.e. normalizing both inputs) abolished seeking behavior (Fig. 5a, b). To examine the persistence of this effect, the same mice were tested for cue-associated cocaine seeking one week later without further optogenetic intervention. Seeking behavior remained absent in mice that received the 13 Hz mPFC protocol (Extended Data Fig. 8a, b, and Extended Data Fig. 9). Taken together, these data demonstrate that cocaine-evoked plasticity at two inputs onto NAc D1R-MSNs are required for the complete expression of cue-associated seeking, while each form of contrasting plasticity is causally related to a different component of the seeking behavior, namely the vigor of the seeking response and the ability to discriminate cocaine from non cocaine directed actions.

Additional tests were performed to control for the behavioral specificity of optogenetic interventions. First, optogenetic removal of cocaine-evoked plasticity did not preclude the

acquisition of further reward-related instrumental learning (Extended Data Fig. 8c, which includes further description). Second, the 13 Hz mPFC protocol did not affect cue-associated food seeking behavior in a cohort of mice that were previously trained to self-administer sucrose pellets (Extended Data Fig. 8d-f, which includes further description), suggesting that this protocol is selective for cocaine-evoked plasticity necessary for cocaine seeking against plasticity that may correlate with food seeking(Counotte et al., 2013; D. G. Smith and Robbins, 2013).

.

## DISCUSSION

A striking feature of this study is the input-specific expression mechanism of drug-evoked plasticity. Within the same D1R-MSN, synapses that belong to the mPFC input show rectifying AMPAR-EPSCs reflecting the insertion of GluA2-lacking CP-AMPARs, while at neighbouring vHipp synapses an increased A/N ratio along with significantly larger EPSC amplitude indicates the insertion of more GluA2-containing AMPARs. Moreover, such forms of plasticity were absent at other synapses and in D2R-MSNs, although these neurons may still contribute to features of addiction(Bock et al., 2013). Why are some synapses susceptible to cocaine-evoked plasticity and why do the expression mechanisms differ between inputs? These findings may reflect a complex induction process, requiring specific neuronal activity patterns coinciding with high levels of mesolimbic dopamine during drug exposure. Indeed, different drug self-administration histories may favour the induction of synaptic plasticity at other NAc inputs, like the BLA(Lee et al., 2013). Another possibility is that contrasting expression mechanisms reflect differences in the quality of basal synaptic transmission between cortical and limbic inputs onto NAc MSNs(Britt et al., 2012), or differences in the sensitivity of synapses to be influenced by the coincidence of converging glutamate and dopamine signals involving D1R signalling(Goto and Grace, 2008; 2005).

Here we focus on the vHipp and mPFC input onto D1R-MSNs taking advantage of endogenous depression mechanisms (e.g. NMDAR or mGluR activation
(Kombian and Malenka, 1994; pascoli et al., 2011; Robbe et al., 2002)) to restore normal transmission in each input separately or both inputs together. While the 1 Hz LTD protocol is sufficient to recruit NMDARs on the activated input, trains of action potentials (e.g. 13 Hz stimulation) are required to release sufficient amounts of glutamate to activate perisynaptically located mGluRs, even at neighbouring inputs. mGluR-LTD in the NAc is expressed both pre- and postsynaptically(Grueter et al., 2010; Mccutcheon et al., 2011; Robbe et al., 2002), but what most likely matters is that mGluR-LTD is an efficient mechanism to remove GluA2-lacking AMPARs, just as in other CNS synapses
(Clem and Huganir, 2010; Grueter et al., 2010; Lüscher and Huber, 2010). It is therefore not surprising that the 1 Hz mPFC protocol failed to normalize RI and had no behavioral effect. The 1 Hz vHipp protocol normalized the A/N ratio at vHipp to D1R-MSN synapses and significantly reduced the vigor with which the animal pressed the active lever in search of cocaine. Thus, cocaine-evoked plasticity at vHipp afferents to NAc D1R-MSNs may enhance recognition of the correct context in which cocaine can be obtained. In the absence of this plasticity, context recognition may be impaired and the certainty of actions reduced. Meanwhile, removal of CP-AMPARs from mPFC to D1R-MSN synapses led to a failure of discrimination between the cocaine-associated lever and a second lever on which responding had no consequence. This establishes cocaine-evoked plasticity at mPFC afferents to NAc D1R-MSNs as necessary to permit correct action-outcome selection during seeking. Finally, restoring transmission in both inputs abolished cue-induced cocaine seeking. Thus, cocaine-evoked plasticity at multiple inputs, with distinct expression mechanisms that change both

the efficacy and quality of transmission, are collectively necessary for the full expression of cue-associated drug seeking behavior.

Previous studies have recognized the importance of NAc excitatory transmission in drug-adaptive behaviors using systemic or local applications of pharmacological agents that are active during the behavioral test (Bellone and Lüscher, 2006; Conrad et al., 2008; Cornish and Kalivas, 2000; Koya et al., 2008). However, a key difference in the present study is that optogenetic protocols were applied outside of the test and remained effective one week later. Thus, findings here provide support for a model whereby a cocaine memory trace commandeers accumbal integration to control core components of relapse. Co-opting endogenous plasticity mechanisms emerges as a radically new way to modify behavior and may serve as a blueprint for defining synaptic causalities in other synaptic disorders.

## REFERENCES


Ambroggi, F., Turiault, M., Milet, A., Deroche-Gamonet, V., Parnaudeau, S., Balado, E., Barik, J., van der Veen, R., Maroteaux, G., Lemberger, T., Schütz, G., Lazar, M., Marinelli, M., Piazza, P.V., Tronche, F., 2009. Stress and addiction: glucocorticoid receptor in dopaminoceptive neurons facilitates cocaine seeking. *Nat Neurosci* **12**, 247–249. doi:10.1038/nn.2282

Bellone, C., Lüscher, C., 2006. Cocaine triggered AMPA receptor redistribution is reversed in vivo by mGluR-dependent long-term depression. *Nat Neurosci* **9**, 636–641. doi:10.1038/nn1682

Berridge, K.C., Kringelbach, M.L., 2013. Neuroscience of affect: brain mechanisms of pleasure and displeasure. *Curr Opin Neurobiol* **23**, 294–303. doi:10.1016/j.conb.2013.01.017

Bertran-Gonzalez, J. Bosch, C. Maroteaux, M., Matamales, M., Hervé, D., Valjent, E., Girault, J.A. 2008. Opposing patterns of signaling activation in dopamine D1 and D2 receptor-expressing striatal neurons in response to cocaine and haloperidol. *J. Neurosci.* **28,** 5671–5685

Bienenstock, E.L., Cooper, L.N., Munro, P.W., 1982. Theory for the development of neuron selectivity: orientation specificity and binocular interaction in visual cortex. *J Neurosci* **2**, 32–48.

Bock, R., Shin, J.H., Kaplan, A.R., Dobi, A., Markey, E., Kramer, P.F., Gremel, C.M., Christensen, C.H., Adrover, M.F., Alvarez, V.A., 2013. Strengthening the accumbal indirect pathway promotes resilience to compulsive cocaine use. *Nat Neurosci* **16**, 632-8 Group 1–9. doi:10.1038/nn.3369

Britt, J.P., Benaliouad, F., McDevitt, R.A., Stuber, G.D., Wise, R.A., Bonci, A., 2012. Synaptic and Behavioral Profile of Multiple Glutamatergic Inputs to the Nucleus Accumbens. *Neuron* **76**, 790–803. doi:10.1016/j.neuron.2012.09.040

Cerovic, M., d'Isa, R., Tonini, R., Brambilla, R., 2013. Neurobiology of Learning and Memory. *Neurobiol Learn Mem* 1–18. doi:10.1016/j.nlm.2013.06.013

Christyakov, V.S, Tsibulsky, V.L., 2006. Intravenous Drug Self-administration in Mice: Practical Considerations. *Behav Genet* **37,** 101–118

Clem, R.L., Huganir, R.L., 2010. Calcium-permeable AMPA receptor dynamics mediate fear memory erasure. *Science* **330**, 1108–1112. doi:10.1126/science.1195298

Conrad, K.L., Tseng, K.Y., Uejima, J.L., Reimers, J.M., Heng, L.-J., Shaham, Y., Marinelli, M., Wolf, M.E., 2008. Formation of accumbens GluR2-lacking AMPA receptors mediates incubation of cocaine craving. *Nature* **454**, 118–121. doi:10.1038/nature06995

Cornish, J.L., Kalivas, P.W., 2000. Glutamate transmission in the nucleus accumbens mediates relapse in cocaine addiction. *J Neurosci* **20**, RC89.

Counotte, D.S., Schiefer, C., Shaham, Y., O'donnell, P., 2013. Time-dependent decreases in nucleus accumbens AMPA/NMDA ratio and incubation of sucrose craving in adolescent and adult rats. *Psychopharmacology*. doi:10.1007/s00213-013-3294-3

DiChiara, G., Bassareo, V., 2007. Reward system and addiction: what dopamine does and doesn't do. *Curr Opin Pharmacol* **7**, 69–76. doi:10.1016/j.coph.2006.11.003

Everitt, B.J., Robbins, T.W., 2005. Neural systems of reinforcement for drug addiction: from actions to habits to compulsion. *Nat Neurosci* **8**, 1481–1489. doi:10.1016/j.neuropharm.2004.06.027

Franklin, K. B. J., & Paxinos, G. The mouse brain in stereotaxic coordinates, Compact 3rd ed. London: Elsevier Academic Press. (2008)

French, S.J., Totterdell, S., 2003. Individual nucleus accumbens-projection neurons receive both basolateral amygdala and ventral subicular afferents in rats. *Neuroscience* **119**, 19–

31. doi:10.1016/S0306-4522(03)00150-7

French, S.J., Totterdell, S., 2002. Hippocampal and prefrontal cortical inputs monosynaptically converge with individual projection neurons of the nucleus accumbens. *J Comp Neurol* **446**, 151–165. doi:10.1002/(SICI)1096-9861(19960108)364:2<340::AID-CNE11>3.0.CO;2-T

Freund, T.F., Powell, J.F., Smith, A.D., 1984. Tyrosine hydroxylase-immunoreactive boutons in synaptic contact with identified striatonigral neurons, with particular reference to dendritic spines. *Neuroscience* **13**, 1189–1215.

Gangarossa, G., Espallergues, J., de Kerchove d'Exaerde, A., El Mestikawy, S., Gerfen, C.R., Hervé, D., Girault, J.A., Valjent, E., 2013. Distribution and compartmental organization of GABAergic medium-sized spiny neurons in the mouse nucleus accumbens. *Front Neural Circuits*. doi:10.3389/fncir.2013.00022/abstract

Gipson, C.D., Kupchik, Y.M., Shen, H., Reissner, K.J., Thomas, C.A., Kalivas, P.W., 2013. Relapse induced by cues predicting cocaine depends on rapid, transient synaptic potentiation. *Neuron* **77,** 867–872

Goto, Y., Grace, A.A., 2008. Limbic and cortical information processing in the nucleus accumbens. *Trends Neurosci* **31**, 552–558. doi:10.1016/j.tins.2008.08.002

Goto, Y., Grace, A.A., 2005. Dopamine-Dependent Interactions between Limbic and Prefrontal Cortical Plasticity in the Nucleus Accumbens: Disruption by Cocaine Sensitization. *Neuron* **47**, 255–266. doi:10.1016/j.neuron.2005.06.017

Grueter, B.A., Brasnjo, G., Malenka, R.C., 2010. Postsynaptic TRPV1 triggers cell type--specific long-term depression in the nucleus accumbens. *Nat Neurosci* **13**, 1519–1525. doi:10.1038/nn.2685

Humphries, M.D., Prescott, T.J., 2010. The ventral basal ganglia, a selection mechanism at the crossroads of space, strategy, and reward. *Prog Neurobiol* **90**, 385–417. doi:10.1016/j.pneurobio.2009.11.003

Hyman, S.E., 2005. Addiction: a disease of learning and memory. *Am J Psychiatry* **162**, 1414–1422. doi:10.1176/appi.ajp.162.8.1414

Kalivas, P.W., Volkow, N.D., 2005. The neural basis of addiction: a pathology of motivation and choice. *Am J Psychiatry* **162**, 1403–1413. doi:10.1176/appi.ajp.162.8.1403

Kasanetz, F., Deroche-Gamonet, V., Berson, N., Balado, E., Lafourcade, M., Manzoni, O., Piazza, P.V., 2010. Transition to Addiction Is Associated with a Persistent Impairment in Synaptic Plasticity. *Science* **328**, 1709–1712. doi:10.1126/science.1187801

Kombian, S.B., Malenka, R.C., 1994. Simultaneous LTP of non-NMDA- and LTD of NMDA-receptor-mediated responses in the nucleus accumbens. *Nature* **368**, 242–246. doi:10.1038/368242a0

Kourrich, S., Rothwell, P.E., Klug, J.R., Thomas, M.J., 2007. Cocaine Experience Controls Bidirectional Synaptic Plasticity in the Nucleus Accumbens. *J Neurosci* **27**, 7921–7928. doi:10.1523/JNEUROSCI.1859-07.2007

Koya, E., Uejima, J.L., Wihbey, K.A., Bossert, J.M., Hope, B.T., Shaham, Y., 2008. Role of ventral medial prefrontal cortex in incubation of cocaine craving. *Neuropharmacology* 1–9. doi:10.1016/j.neuropharm.2008.04.022

Lee, B.R., Ma, Y.-Y., Huang, Y.H., Wang, X., Otaka, M., Ishikawa, M., Neumann, P.A., Graziane, N.M., Brown, T.E., Suska, A., Guo, C., Lobo, M.K., Sesack, S.R., Wolf, M.E., Nestler, E.J., Shaham, Y., Schlüter, O.M., Dong, Y., 2013. Maturation of silent synapses in amygdala-accumbens projection contributes to incubation of cocaine craving. *Nat Neurosci* doi:10.1038/nn.3533

Liu, S.J., Zukin, R.S., 2007. Ca2+-permeable AMPA receptors in synaptic plasticity and neuronal death. *Trends Neurosci* **30**, 126–134. doi:10.1016/j.tins.2007.01.006

Lüscher, C., Huber, K.M., 2010. Group 1 mGluR-Dependent Synaptic Long-Term Depression: Mechanisms and Implicationsfor Circuitry and Disease. *Neuron* **65**, 445–459. doi:10.1016/j.neuron.2010.01.016

Lüscher, C., Malenka, R.C., 2012. NMDA Receptor-Dependent Long-Term Potentiation and Long-Term Depression (LTP/LTD). *Cold Spring Harb Perspect Biol* **4**, a005710–a005710. doi:10.1101/cshperspect.a005710

Lüscher, C., Malenka, R.C., 2011. Drug-Evoked Synaptic Plasticity in Addiction: From Molecular Changes to Circuit Remodeling. *Neuron* **69**, 650–663. doi:10.1016/j.neuron.2011.01.017

MacAskill, A.F., Little, J.P., Cassel, J.M., Carter, A.G., 2012. Subcellular connectivity underlies pathway-specific signaling in the nucleus accumbens. *Nat Neurosci* **15**, 1624-6. doi:10.1038/nn.3254

Mccutcheon, J.E., Loweth, J.A., Ford, K.A., Marinelli, M., Wolf, M.E., Tseng, K.Y., 2011. Group I mGluR Activation Reverses Cocaine-Induced Accumulation of Calcium-Permeable AMPA Receptors in Nucleus Accumbens Synapses via a Protein Kinase C-Dependent Mechanism. *J Neurosci* **31**, 14536–14541. doi:10.1523/JNEUROSCI.3625-11.2011

Ortinski, P.I., Vassoler, F.M., Carlson, G.C., Pierce, R.C., 2012. Temporally Dependent Changes in Cocaine-Induced Synaptic Plasticity in the Nucleus Accumbens Shell are Reversed by D1-Like Dopamine Receptor Stimulation. *Neuropsychopharmacology* 1–12. doi:10.1038/npp.2012.12

Ouimet, C.C, Miller, P.E., Hemmings, H.C. Jr, Walaas, S.I., Greengard, P., 1984. DARPP-32, a dopamine- and adenosine 3':5'-monophosphate-regulated phosphoprotein enriched in dopamine-innervated brain regions. III. Immunocytochemical localization. *J. Neurosci.* **4** (1), 111-24

Papp, E., Borhegyi, Z., Tomioka, R., Rockland, K.S., Mody, I., Freund, T.F., 2011. Glutamatergic input from specific sources influences the nucleus accumbens-ventral pallidum information flow. *Brain Struct Funct* **217**, 37-48. doi:10.1007/s00429-011-0331-z

Pascoli, V., Turiault, M., Lüscher, C., 2011. Reversal of cocaine-evoked synaptic potentiation resets drug-induced adaptive behaviour. *Nature* **481**, 71–75. doi:10.1038/nature10709

Robbe, D., Kopf, M., Remaury, A., Bockaert, J., Manzoni, O.J., 2002. Endogenous cannabinoids mediate long-term synaptic depression in the nucleus accumbens. *Proc Natl Acad Sci USA* **99**, 8384–8388. doi:10.1073/pnas.122149199

Robbins, T.W., Everitt, B.J., 1996. Neurobehavioural mechanisms of reward and motivation. *Curr Opin Neurobiol* **6**, 228–236.

Saddoris, M.P., Sugam, J.A., Cacciapaglia, F., Carelli, R.M., 2013. Rapid dopamine dynamics in the accumbens core and shell: learning and action. *Front Biosci* (Elite Ed) **5**, 273–288.

Schultz, W., 2011. Potential vulnerabilities of neuronal reward, risk, and decision mechanisms to addictive drugs. *Neuron* **69**, 603–617. doi:10.1016/j.neuron.2011.02.014

Smith, D.G., Robbins, T.W., 2013. The Neurobiological Underpinnings of Obesity andBinge Eating: A Rationale for Adopting the FoodAddiction Model. *Biol Psychiatry* **73**, 804–810. doi:10.1016/j.biopsych.2012.08.026

Smith, R.J., Lobo, M.K., Spencer, S., Kalivas, P.W., 2013. Cocaine-induced adaptations in D1 and D2 accumbens projection neurons (a dichotomy not necessarily synonymous with direct and indirect pathways). *Curr Opin Neurobiol* **23**, 546-52 doi:10.1016/j.conb.2013.01.026

Sparta, D.R., Stamatakis, A.M., Phillips, J.L., Hovelsø, N., van Zessen, R.,Stuber, G.D. 2011. Construction of implantable optical fibers for long-term optogenetic manipulation of neural circuits. *Nat Protoc* **7,** 12–23

Thomsen, M., Caine S.B. 2006. Intravenous Drug Self-administration in Mice: Practical Considerations. *Behav Genet* **37,** 101–118

**Acknowledgments** We thank Daniel Huber and Matthew Brown as well the members of the Lüscher lab for discussion and comments on the manuscript, and Agnes Hiver for assisting in animal surgery. This work was funded by a grant of the Swiss National Science Foundation, the National Center of Competence in Research (NCCR) "SYNAPSY - The Synaptic Bases of Mental Diseases" of the Swiss National Science Foundation and ERC advanced grant (MeSSI). J.T. is supported by a MD-PhD grant of the Swiss Confederation.

**Author contributions** V.P. performed all the *in vitro* electrophysiological recordings. J.T. performed all surgery and behavioral experiments with the assistance of E.C.O'C. J.E. and E.V. performed the fluorescence immunohistochemical experiments. C.L., P.V., J.T. and E.C.O'C. designed the study, and C.L. wrote the manuscript with the help of all authors.

**Author Information** Reprints and permissions information is available at www.nature.com/reprints. The authors declare no competing financial interests. Readers are welcome to comment on the online version of this article at www.nature.com/nature. Correspondence and requests for materials should be addressed to C.L. (christian.luscher@unige.ch).

**Figure 1. Withdrawal from cocaine self-administration evokes cell-type specific modifications of excitatory synapses in the NAc. a.** Raster plot for infusions, active and inactive lever presses in a function of time during acquisition of self-administration (SA) for a saline (top) or cocaine (bottom) SA mouse. **b.** Mean total lever presses (top) and infusions (bottom) during the acquisition phase of saline (n = 42) or cocaine (n = 164) SA for all mice used in the study. **c.** Schematic of experiment (top). Sample traces of AMPAR-EPSCs at -70, 0, and +40 mV (colored) and NMDAR-EPSCs at +40 mV (black) (bottom), and plots (right) of AMPA/NMDA (A/N) ratio as a function of rectification index (RI; small dots) for each D1R- (n=9/41, saline/cocaine) or D2R-MSN (n=8/25). Large open and filled dots represent group mean saline and cocaine data, respectively. Cocaine increased RI and A/N ratio in D1R-MSNs but not in D2R-MSNs (RI in D1R- and D2R-MSNs: effect of group (cocaine/saline), $F_{1,83} = 10.86$, $P < 0.01$; cell type x group, $F_{1,83} = 6.08$, $P < 0.05$. Student's *t*-test for cocaine vs. saline in D1R-MSNs, $t_{48} = 3.72$, $^{*}P < 0.01$; in D2R-MSNs, $t_{31} = 0.80$, $P = 0.43$. A/N ratio in D1R- and D2R-MSNs: effect of group, $F_{1,83} = 5.91$, $P < 0.05$; cell type x group, $F_{1,83} = 8.34$, $P < 0.01$. Student's *t*-test for cocaine vs. saline in D1R-MSNs, $t_{48} = 3.25$, $^{\#}P < 0.01$, in D2R-MSNs, $t_{31} = 0.62$, $P = 0.54$). Scale bars: 20 pA, 20 ms. Plots show means with s.e.m.

**Figure 2. Withdrawal from cocaine self-administration evokes input-specific plasticity in NAc D1R-MSNs. a.** Top, images of BLA: basolateral amygdala; vHipp: ventral subiculum of the hippocampus; mPFC: medial prefrontal cortex infected with ChR2-eYFP, with example traces and mean peak amplitudes of photo-currents (100 ms light pulses). Scale bars: 50 ms, 50 pA. Bottom, confocal image of NAc shell from a Drd1a-tdTomato mouse infected with ChR2 in the mPFC, as used for input and cell-type specific recordings. Cell nuclei are stained with Hoechst. Scale bar: 100 μm. **b.** Top, schematic of whole-cell recordings of D1R-MSNs from mice infected with ChR2 in the BLA (left), vHipp (center) or mPFC (right). Bottom, cocaine SA increased the mean amplitude of 4 ms light-evoked EPSCs at vHipp and mPFC synapses ($t_{62} = 3.12$, $^{*}P < 0.01$, n = 30/34 for saline/cocaine and $t_{120} = 3.0$, $^{*}P < 0.01$, n = 66/56, respectively), but did not change BLA synapses ($t_{18} = 0.88$, $P = 0.39$; n = 11/9). **c.** For each input, example traces are shown (top), with I/V plots (bottom) and group mean RI data (right). Cocaine decreased normalized AMPAR-EPSCs at +40 mV from mPFC ($t_{19} = 4.16$, $P < 0.01$, n = 8/13 for saline/cocaine) but not from BLA or vHipp inputs ($t_{11} = 0.67$, $P = 0.52$, n = 5/8 and $t_{20} = 0.18$, $P = 0.86$, n = 9/13 respectively). The RI was increased at mPFC synapses ($t_{19} = 6.9$, $^{*}P \leq 0.001$), but not at BLA or vHipp synapses ($t_{11} = 0.58$, $P = 0.57$ and $t_{20} = 0.22$, $P = 0.83$, respectively). Scale bars: 20 ms, 20 pA. **d.** The A/N ratio was decreased by cocaine SA at mPFC synapses ($t_{19} = -3.59$, $P < 0.01$), but increased at vHipp synapses ($t_{20} = 8.33$, $P < 0.001$) and unchanged at BLA synapses ($t_{11} = 0.94$, $P = 0.36$). $^{*}P < 0.05$. Scale bars: 20 ms, 20 pA. Error bars show s.e.m.

**Figure 3. Homosynaptic effects of optogenetic protocols applied *ex vivo* on D1R-MSN plasticity a.** Schematic of experiment for panels b-e; ChR2 in vHipp **b.** Graph of normalized light-evoked EPSCs across time (bottom: each point represents mean of 6 sweeps), with example traces (top: mean of 20 sweeps) before (1) and after (2) the LTD protocol (4 ms pulses at 1 Hz, 10 min). One month after cocaine SA, the efficiency of the 1 Hz LTD

protocol was not modified (56.3 ± 14.7% to 38.6 ± 12.2%, $t_7 = 0.89$, $P = 0.4$; n = 5/4). **c.** As for panel b, but with a 13 Hz protocol (4 ms pulses at 13 Hz, 10 min). The efficiency of this protocol was reduced in cocaine SA mice (39.2 ± 6.7% to 69.5 ± 10.1%, $t_9 = 2.57$, $P = 0.03$; n = 6/5). **d.** Example traces (left) of light-evoked AMPAR-EPSCs recorded at -70, 0 and +40 mV, with I/V plot (middle) and group mean RI data (right) before (Ctrl) and after the 1 or 13 Hz light protocol, in both saline (s) and cocaine (c) SA groups. AMPAR composition was not modified by cocaine or light protocols (saline/cocaine for Ctrl (n = 9/13), 1 Hz (6/4), 13 Hz (8/5)). **e.** For the same cells in panel d, example traces (left), with mean A/N ratios (right) before or after the 1 or 13 Hz protocol. Planned comparisons, following ANOVA, by *t*-test, $^{o,*}P \leq 0.05$ **f.** Schematic of experiment for panels g-j; ChR2 in the mPFC. **g.** The 1 Hz protocol efficiency was reduced in cocaine SA mice (43 ± 5.5% to 74 ± 3.7%, $t_{17} = 4.9$, $^{*}P < 0.001$; n = 8/11). **h.** The 13 Hz protocol efficiency was increased in cocaine SA mice (54 ± 6.1% to 29 ± 4.7%, $t_{22} = 3.25$, $^{*}P < 0.01$; n = 13/11). **i.** The 13 Hz but not 1 Hz protocol normalized cocaine-evoked changes in AMPAR-EPSCs at +40 mV and RI. Planned comparisons, following ANOVA, by *t*-test, $^{o,*}P \leq 0.05$; (saline/cocaine for Ctrl (n = 9/13), 1 Hz (10/7), 13 Hz (10/6)). **j.** For the same cells as panel i, the cocaine-evoked decrease in A/N ratio was normalized by the 13 Hz, but not the 1 Hz protocol. The 1 Hz protocol decreased A/N ratio in saline mice. Planned comparisons, following ANOVA, by *t*-test, $^{o,*}P \leq 0.05$. Note that Ctrl data is the same as shown in Fig 2. Error bars show s.e.m.

**Figure 4. Heterosynaptic effects of optogenetic protocols applied *ex vivo* on D1R-MSN plasticity a.** Schematic of experiment. **b.** Example traces (left) of electrically-evoked AMPAR-EPSCs recorded at -70, 0 and +40 mV, with I/V plots (middle) and grouped mean RI data (right) before (Ctrl) or after light protocols (1 or 13 Hz) were applied with ChR2 in the vHipp or mPFC. The 13 Hz but not 1 Hz light protocol applied at vHipp or mPFC synapses normalized AMPA-EPSCs at +40 mV and RI (planned comparisons, following ANOVAs, with *t*-tests: $^{*}P \leq 0.05$; (saline/cocaine for Ctrl (n = 9/41), for vHipp 1 Hz (6/8) and 13 Hz (8/8), for mPFC 1 Hz (12/9) and 13 Hz (15/8)). **c.** For the same cells shown in panel b, example traces (left) and group mean A/N ratios (right) before or after the 1 or 13 Hz protocols. The 1 Hz vHipp or the 13 Hz mPFC protocol normalized the cocaine-evoked increase in A/N ratio, while the A/N ratio remained elevated following the 13 Hz vHipp protocol or the 1 Hz mPFC protocol (planned comparisons, following ANOVAs, with *t*-tests: $^{*}P < 0.05$ and $^{\#}P = 0.07$). Note that Ctrl data is the same as shown in Fig 1. Error bars show s.e.m.

**Figure 5. Linking cocaine-evoked plasticity at identified inputs to specific components of cue-associated cocaine seeking. a.** Raster plots showing active and inactive lever presses during a cue-associated seeking session **b.** Group mean data showing active (a) and inactive (i) lever presses. Seeking was robust in cocaine SA control mice (active vs. inactive lever, $t_{43} = 9.5$, $^{\#}P < 0.001$; n = 11/44, saline/cocaine; active lever to saline control group, following ANOVA, by *t*-test: $t_{53} = 4.6$, $^{*}P < 0.001$). Seeking was present following the 1 Hz vHipp protocol ($t_{10} = 3.6$, $^{\#}P < 0.01$), but active lever responses were significantly

diminished (vs. cocaine control group, following ANOVA, by *t*-test: $t_{53} = 2.3$, $^{o}P < 0.05$; n = 11/44). Lever discrimination was lost following the 13 Hz vHipp protocol ($t_8 = 1.99$, $P > 0.05$), and inactive lever responses were significantly increased (vs. cocaine control group, following ANOVA, by *t*-test: $t_{51} = 4.48$, $^{\#}P < 0.001$; n = 9/44). Seeking was present following the 1 Hz mPFC protocol and did not differ from the cocaine controls (vs. cocaine control groups by ANOVA: lever, protocol and lever x protocol interaction all n.s.; n = 11/44). Active lever responding was reduced following the 13 Hz mPFC protocol (vs. cocaine control group, following ANOVA, by *t*-test: $t_{52} = 4.3$, $^{o}P < 0.001$; n = 10/44) and lever discrimination was lost (active vs. inactive levers by t-test, $t_9 = 1.7$, $P > 0.1$, n = 10). See Extended Data table 1 for complete statistics. Error bars show s.e.m.

## Supplementary References


44. Franklin, K. B. J., & Paxinos, G. The mouse brain in stereotaxic coordinates, Compact 3rd ed. London: Elsevier Academic Press. (2008)
45. Bertran-Gonzalez, J. *et al.* Opposing patterns of signaling activation in dopamine D1 and D2 receptor-expressing striatal neurons in response to cocaine and haloperidol. *J. Neurosci.* **28,** 5671–5685 (2008).
46. Ouimet CC., *et al.* DARPP-32, a dopamine- and adenosine 3':5'-monophosphate-regulated phosphoprotein enriched in dopamine-innervated brain regions. III. Immunocytochemical localization. *J. Neurosci.* **4** (1), 111-24 (1984)
47. Thomsen, M. & Caine, S. B. Intravenous Drug Self-administration in Mice: Practical Considerations. *Behav Genet* **37,** 101–118 (2006).
48. Chistyakov, V. S. & Tsibulsky, V. L. How to achieve chronic intravenous drug self-administration in mice. *J Pharmacol Toxicol Methods* **53,** 117–127 (2006).
49. Gipson, C. D. *et al.* Relapse induced by cues predicting cocaine depends on rapid, transient synaptic potentiation. *Neuron* **77,** 867–872 (2013).
50. Sparta, D. R. *et al.* Construction of implantable optical fibers for long-term optogenetic manipulation of neural circuits. *Nat Protoc* **7,** 12–23 (2011).

**Extended Data Figure 1. Graphical abstract.** Top left: main excitatory afferents onto NAc shell D1R-MSNs (BLA: basolateral amygdala, vHipp: ventral subiculum of the hippocampus and mPFC: medial prefrontal cortex), which at baseline contain synapses that express NMDARs and GluA2-containing AMPARs. Top right: one month following withdrawal (WD) from cocaine self-administration (SA), mPFC synapses onto NAc shell D1R-MSNs express GluA2-lacking AMPARs while more GluA2-containing AMPARs are added at vHipp synapses. Effects of NMDAR-dependent or mGluR1-dependent (1 or 13 Hz, respectively) light protocols applied at specific inputs (shown in green) on cocaine-evoked plasticity are illustrated, together with the consequence for cue-associated seeking behavior.

**Extended Data Figure 2. Identification and optogenetic targeting of excitatory inputs to the NAc shell**. **a**. Retrograde labelling with cholera toxin subunit B (CTB, AF594) injected into the NAc shell. Confocal images of injection sites (top) in the medo-dorsal (left) and medio-ventral (right) NAc shell are shown, regions where electrophysiology recordings were performed. **b.** Labelled cell bodies in corresponding projection areas (basolateral amygdala, ventral subiculum of the hippocampus and medial prefrontal cortex) are shown, with no discernable segregation between the medio-dorsal or medio-ventral NAc shell. For each projection area, the insert shows a complete hemisphere coronal section together with a zoomed image of the region of interest (indicated by yellow box). Il: Infralimbic; CeL; Central Amygdala Lateral; BLP: Basolateral Amydala posterior; BMP: Basomedial amygdala posterior; PV: paraventricular thalamic nucleus; vHipp: central subiculum of the hippocampus; VIEnt: Ventral intermediate entorhinal cortex; VTA: Ventral tegmental area. **c**. Schematic of experiment (top) with light-evoked EPSCs recorded in D1R-MSNs of the NAc shell of mice infected with AAV1-ChR2-eYFP in the BLA (bottom left), vHipp (middle) or vmPFC (right) before and after bath application of glutamate receptor antagonists (NBQX 10 μM and AP5 50 μM for AMPAR and NMDAR, respectively). Scale bars: 20 ms, 50 pA

**Extended Data Figure 3. Individual MSNs receive inputs from multiple projection areas**. **a.** Confocal images of NAc from a mouse infected with AAV5-EF1-eYFP and AAV5-EF1-mCherry in the vHipp (left) and mPFC (right), respectively, at low magnification (first row). At higher magnification (second and third row) eYFP from vHipp and mCherry from mPFC are present around MSNs stained by DARPP-32 (blue). aca, anterior commissure. Scale bar: 50 μm.

**Extended Data Figure 4. Cocaine SA does not evoke input-specific plasticity in D2R-MSNs**. **a**. Top, schematic of whole-cell recordings of NAc shell D2R-MSNs of mice that one month previously self-administered saline (open points) or cocaine (filled points) and were infected with AAV1-ChR2-eYFP in the BLA (left), vHipp (middle) or mPFC (right). Bottom, following cocaine SA the mean amplitude of light evoked EPSCs was not changed at any input onto D2R-MSNs (effect of group (saline/cocaine) and group x input (BLA/vHipp/mPFC) all not significant). n = 10/14 for BLA (saline/cocaine), n = 10/20 for vHipp and n = 60/51 for mPFC. **b.** For each input, the rectification index (RI) was calculated. Example traces are shown (top), with the I/V plot (middle) and group mean RI

data (bottom). Cocaine did not modify normalized AMPAR-EPSCs at +40 mV from BLA, vHipp or mPFC inputs ($t_{12}$ = -0.20, $P$ = 0.84, $t_{18}$ = 0.44, $P$ = 0.67 and $t_{20}$=0.43, $P$ = 067, respectively). The RI was also unchanged at D2R-MSN synapses from BLA, vHipp or mPFC inputs ($t_{12}$ = -0.32, $P$ = 0.75, $t_{18}$ = -0.51, $P$ = 0.62 and $t_{20}$ = -0.67, $P$ = 0.51 respectively). Scale bars: 20 ms, 20 pA. **c**. For the same cells as shown in panel b, the A/N ratio was calculated. For each input, example traces are shown (top), with group mean A/N ratios (bottom). Cocaine did not alter the A/N ratio at inputs onto D2R-MSNs from the BLA, vHipp or mPFC ($t_{12}$ = -0.19, $P$ = 0.85, $t_{18}$ = 1.20, $P$ = 0.25 and $t_{20}$ = -0.04, $P$ = 0.97, respectively). Scale bars: 20 ms, 20 pA. Error bars show s.e.m.

**Extended Data Figure 5. mPFC and NAc recordings during 1 and 13 Hz optogenetic protocols and LTD in NAc D2R-MSNs induced by mPFC protocols applied after saline and cocaine SA**. **a.** Right, schematic of whole-cell recordings in the mPFC or NAc from mice infected with ChR2 in mPFC. Top, light-evoked action potentials recorded in current clamp of ChR2 infected mPFC neurons and EPSCs recorded in voltage-clamp of D1R-MSNs (bottom) during the beginning of the 1 Hz (left) or 13 Hz (right) stimulation protocols. Note that EPSCs fail to follow the 13 Hz protocol. **b.** Top left, schematic of experiment. Bottom, graph of normalized light evoked EPSCs across time recorded in NAc D2R-MSNs from saline and cocaine SA mice (each point represents mean of 6 sweeps), together with example traces (mean of 20 sweeps) before (1) and after (2) a 1 (left) or 13 Hz (right) light protocol was applied *ex vivo* (4 ms pulses at 1 or 13 Hz, 10 min). One month after saline or cocaine SA, the 1 Hz and 13 Hz protocols induced comparable LTDs in both groups (for 1 Hz: 50 ± 4.9% to 40 ± 2.6%, Student's t-test $t_{14}$ = -1.86, $P$ = 0.080; n = 7-9 cells; for 13 Hz: 28 ± 3.7% to 33 ± 4.2%, Student's t-test $t_{18}$ = 1.41, $P$ = 0.18; n = 11-9 cells). Error bars show s.e.m.

**Extended Data Figure 6. Optogenetic protocols applied *in vivo* reverse cocaine evoked-plasticity at NAc D1R-MSNs. a.** Top, schematic of experiment. Mice were infected with ChR2 in the vHipp or mPFC and trained in saline or cocaine SA. Mice were then implanted with fiber optics targeting the NAc shell and optogenetic protocols were applied *in vivo* one month after withdrawal. Four hours later, acute brain slices were prepared to assess the efficiency of optogenetic protocols applied *in vivo* to reverse cocaine-evoked plasticity at NAc D1R-MSNs. In brief, consistent with the *ex vivo* validation, the 1 Hz vHipp protocol applied *in vivo* normalized the A/N ratio, while the 13 Hz mPFC protocol normalized the IV curve and rectification index in cocaine SA mice. **b.** Left, schematic of experiment indicating that mice were infected with ChR2 in the vHipp. The rectification index (RI) and A/N ratio was determined with light evoked EPSCs as described previously (see main figure 2). The I/V plot is shown, together with group mean RI and A/N data. Cocaine did not alter normalized AMPAR-EPSCs recorded at +40 mV or the RI from vHipp inputs (same data as figure 3). The 1 Hz protocol applied *in vivo* was without effect on either of these measures in saline or cocaine SA mice (effect of group (saline vs. cocaine), protocol (control vs. 1 Hz) and group x protocol, all not significant). The A/N ratio was increased at vHipp inputs in cocaine SA mice (same data as figure 3) an effect that was reduced following the *in vivo* 1 Hz protocol (planned comparison, following ANOVA, by *t*-test, $t_{26}$ = 4.97, $^{o}P < 0.001$). n =

13/15 for 1 Hz saline/cocaine group. **c.** As for panel b, except that mice were infected with ChR2 in the mPFC. Cocaine decreased AMPAR-EPSCs recorded at +40 mV and increased the RI from mPFC inputs (same data as figure 3). The 13 Hz protocol applied *in vivo* increased AMPAR-EPSCs at +40 mV in cocaine SA mice (planned comparison to cocaine control group, following ANOVA, by *t*-test, $t_{20} = 3.6$, $^{o}P < 0.01$) and decreased the R/I in cocaine SA mice (planned comparison to cocaine controls, following ANOVA, by *t*-test, $t_{20} = 5.2$, $^{o}P < 0.001$). The A/N ratio was decreased at mPFC inputs in cocaine SA mice (same data as figure 3), an effect that was normalized following the *in vivo* 13 Hz protocol (planned comparison to cocaine controls, following ANOVA, by *t*-test, $t_{20} = 2.8$, $^{o}P = 0.01$). n = 11/9 for 13 Hz saline/cocaine group. Error bars show s.e.m.

**Extended Data Figure 7. Assessing effects of *in vivo* light stimulation on mEPSCs recorded in D2R- and D1R-MSNs. a.** Top, schematic of experiment. Mice were infected with ChR2 in the vHipp or mPFC and trained in saline or cocaine SA. Mice were then implanted with fiber optics targeting the NAc shell and optogenetic protocols applied *in vivo* one month after withdrawal. Four hours later, acute brain slices were prepared to assess the effect of optogenetic protocols applied *in vivo* on global excitatory transmission by recording mEPSCs at NAc D2R-MSNs. In brief, recordings from D2R-MSNs revealed that mEPSCs were not affected by cocaine and not depressed by optogenetic LTD protocols applied *in vivo*. Note that although optogenetic protocols efficiently induced LTD at single inputs onto D2R-MSNs (Extended Data Fig. 5), this was not reflected by a decrease in mEPSC amplitudes. This may be accounted for by a pre-synaptic expression mechanism of LTD or that baseline amplitudes were already low such that a further depression at only a single input could not be measured by mEPSCs (i.e. floor effect), which reflect synaptic transmission from multiple inputs. **b.** Example of mEPSCs recorded *ex vivo* in NAc shell D2R-MSNs in the presence of picrotoxin (100 μM) and tedrodotoxin (0.5 μM) (sample traces comprising 6 superimposed, 4 sec traces). Scale bars: 20 pA, 500 ms. **c.** Histograms of group mean data of D2R-MSN mEPSC amplitudes (left) and frequency (right) are shown in control saline (sal) or cocaine (coc) conditions and following application of 1 Hz or 13 Hz light protocols at vHipp or mPFC synapses. Mean mEPSC amplitudes and frequencies were not changed by cocaine, and were not significantly decreased by protocols applied at either vHip or mPFC inputs. n = 5 to 13 cells per group. All error bars show s.e.m. **d** and **e** As for panel **a** and **b** except in D1R-MSNs. In brief, the frequency of mEPCS was not affected by cocaine SA or laser protocols. In contrast, in cocaine SA mice the amplitude of mEPSCs was significantly larger than controls, in line with a postsynaptic expression mechanism. Protocols that were most efficient at restoring the A/N ratio at vHipp synapses when assessed on slice, namely the 13 Hz mPFC and the 1 Hz vHipp protocol, were also most efficient at restoring baseline mEPSC amplitudes when applied *in vivo*. This suggests that cocaine-evoked plasticity at vHipp inputs largely accounts for the observed increase in mEPSC amplitudes. **f.** Mean mEPSC amplitudes were increased by cocaine SA (vs. saline control, by *t*-test, $t_{18} = 7.13$, $^{*}P < 0.001$). Protocols applied at vHipp terminals altered mEPSC amplitudes (one-way ANOVA comparing cocaine control, 1 and 13 Hz vHipp protocols: effect of protocol $F_{2,28} = 5.7$, $P < 0.01$). The 1 Hz but not the 13 Hz vHipp protocol reduced mEPSC amplitudes (vs. cocaine control, for 1 Hz: $t_{18} = 2.8$, $^{o}P = 0.01$),

although amplitudes remained significantly higher than saline control mice following either protocol (*P's* < 0.01). Protocols applied at mPFC terminals also altered mEPSC amplitudes (effect of protocol, $F_{2,29} = 13.1$, $P < 0.001$), and the 13 Hz but not 1 Hz mPFC protocol reduced mEPSC amplitudes (vs. cocaine control, for 1 Hz: $t_{19} = 4.7$, $^{o}P < 0.001$). Moreover, amplitudes after the 13 Hz mPFC protocol did not differ from saline controls ($P = 0.14$). The frequency of mEPSCs were not altered by cocaine or by protocols applied at either vHipp or mPFC inputs. n = 8-11 cells per group. All error bars show s.e.m.

**Extended Data Figure 8. Optogenetic effect on cocaine seeking is persistent, and does not alter learning of a new response for food reward or food cue-associated seeking. a.** Schematic of experiment. Cocaine control and 13 Hz mPFC group mice were exposed to a second cocaine cue-associated seeking test one week after the first test (see Fig. 5), but without further optogenetic intervention. Two days after this second test, subgroups of mice from each condition were trained to nose-poke for sucrose pellets during once daily 30 min sessions over 9 days. **b.** Raster plots of cue-associated seeking behavior (active and inactive lever presses) during the second test are shown (left), together with group mean data showing active (a: filled boxes) and inactive (i: open boxes) lever presses. Seeking was present in cocaine control mice during the second test, but was absent in the 13 Hz mPFC group (effect of group, group and lever group, all *P's* < 0.05; active vs. inactive lever comparison by *t*-test, $t_{43} = 6.13$, $^{\#}P < 0.001$ for controls n = 44 and $t_{9} = 0.97$, $P = 0.35$ for 13 Hz mPFC, n = 10; active vs. active lever comparison, $^{o}P < 0.01$). **c.** For the acquisition of a new response test, group mean values are shown of active and inactive nose-pokes across training days. Responding was maintained by FR1, FR2 and FR3 schedules. ANOVA comparisons of nose poke responding across three days at each FR confirmed no difference between cocaine SA control (n = 15) and 13 Hz mPFC (n = 4) mice (Effects of group and day x group x nose poke interactions, all not significant). **d.** Schematic of experiment. One month after food SA training, mice received the 13 Hz mPFC light protocol, 4 h before a 30 min test of seeking. **e.** Graph shows mean of active (a) and inactive (i) lever presses for sucrose pellets by new cohort of mice (n =14) infected or not with ChR2 in the mPFC. Training parameters were identical to those used for the acquisition of cocaine SA, except that sessions lasted only 30 minutes **f.** Raster plots active and inactive lever presses during a cue-associated sucrose seeking session (left), together with group mean data of total active (a) and inactive (i) lever presses during the 30 min seeking test. Food seeking was robust in control mice and did not differ in the 13 Hz mPFC group (effect of lever, $F_{1,12} = 163.7$, $P < 0.002$; group and lever x group all n.s.; n = 6/8). Error bars show s.e.m.

**Extended Data Figure 9. Position of fiber optic cannula placements for mice used in tests of cue-seeking.** Figure shows identified fiber optic cannula tip placements in controls (left) or mice that received different light protocols targeting either vHipp or mPFC to NAc synapses (right). Note that when mice were used for electrophysiology recordings, fiber optic placements were visually confirmed but not recorded.

**Extended Data Table 1. ANOVA comparisons for main figures 1-4 (a) and 5 (b)**

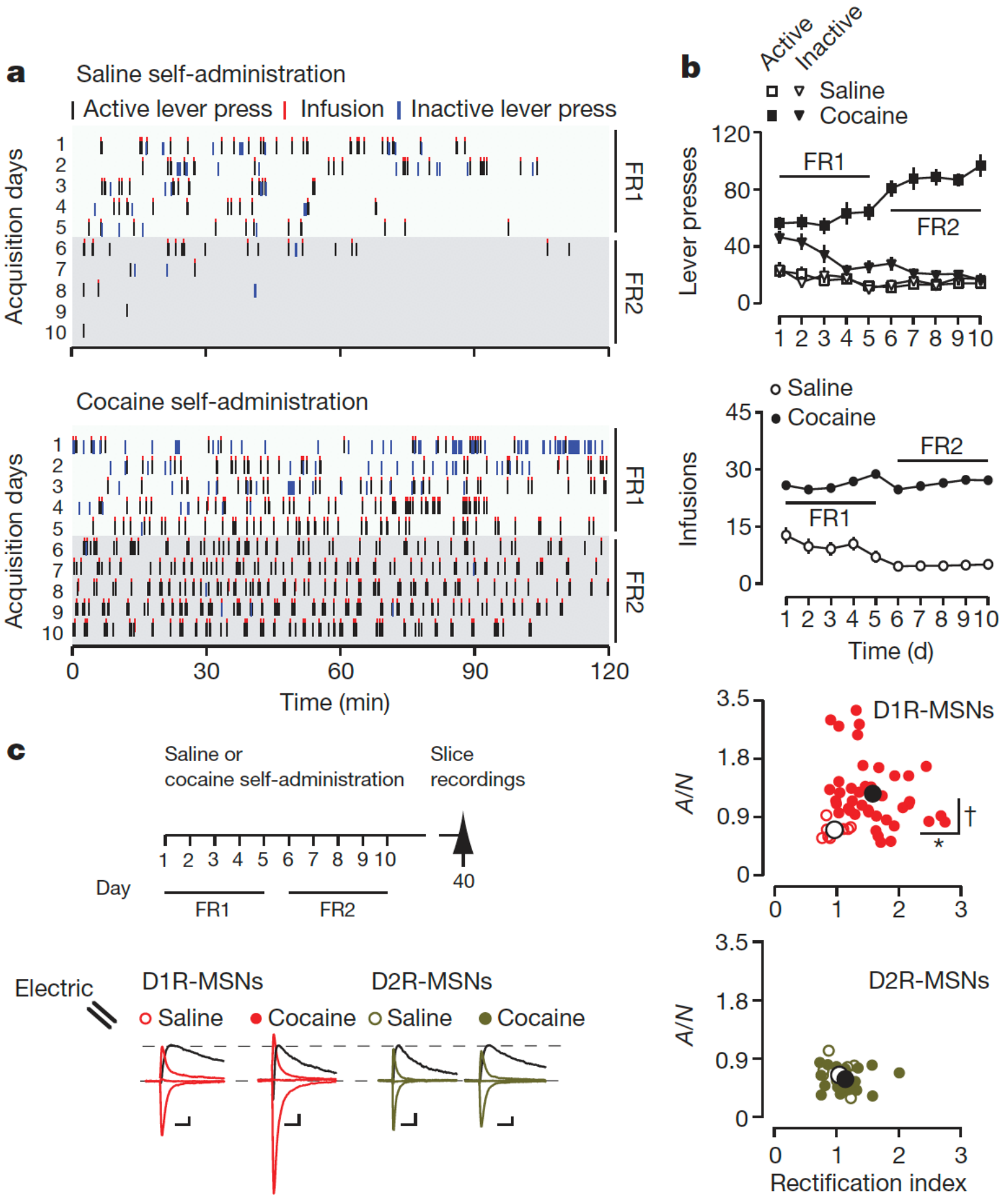
a
Saline self-administration
Active lever press
Infusion
Inactive lever press
Acquisition days
FR1
FR2
Cocaine self-administration
Time (min)
b
Active
Inactive
Saline
Cocaine
Lever presses
Infusions
Time (d)
c
Saline or
cocaine self-administration
Slice
recordings
Day
Electric
D1R-MSNs
D2R-MSNs
A/N
Rectification index

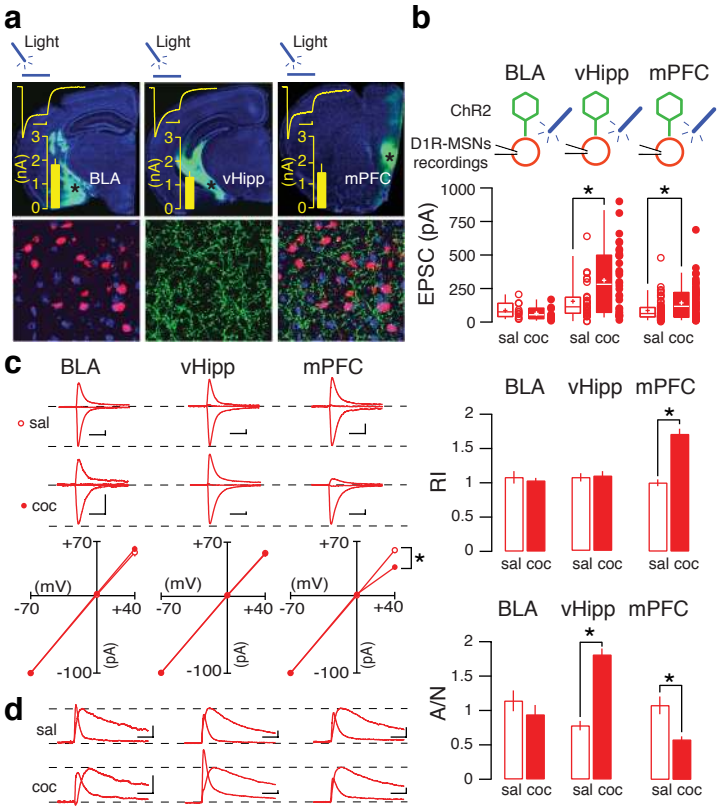
a
Light
Light
Light
BLA
vHipp
mPFC
(nA)
b
BLA
vHipp
mPFC
ChR2
D1R-MSNs
recordings
EPSC (pA)
sal coc
c
BLA
vHipp
mPFC
sal
coc
+70
(mV)
-70
+40
-100
(pA)
RI
A/N
d
sal
coc

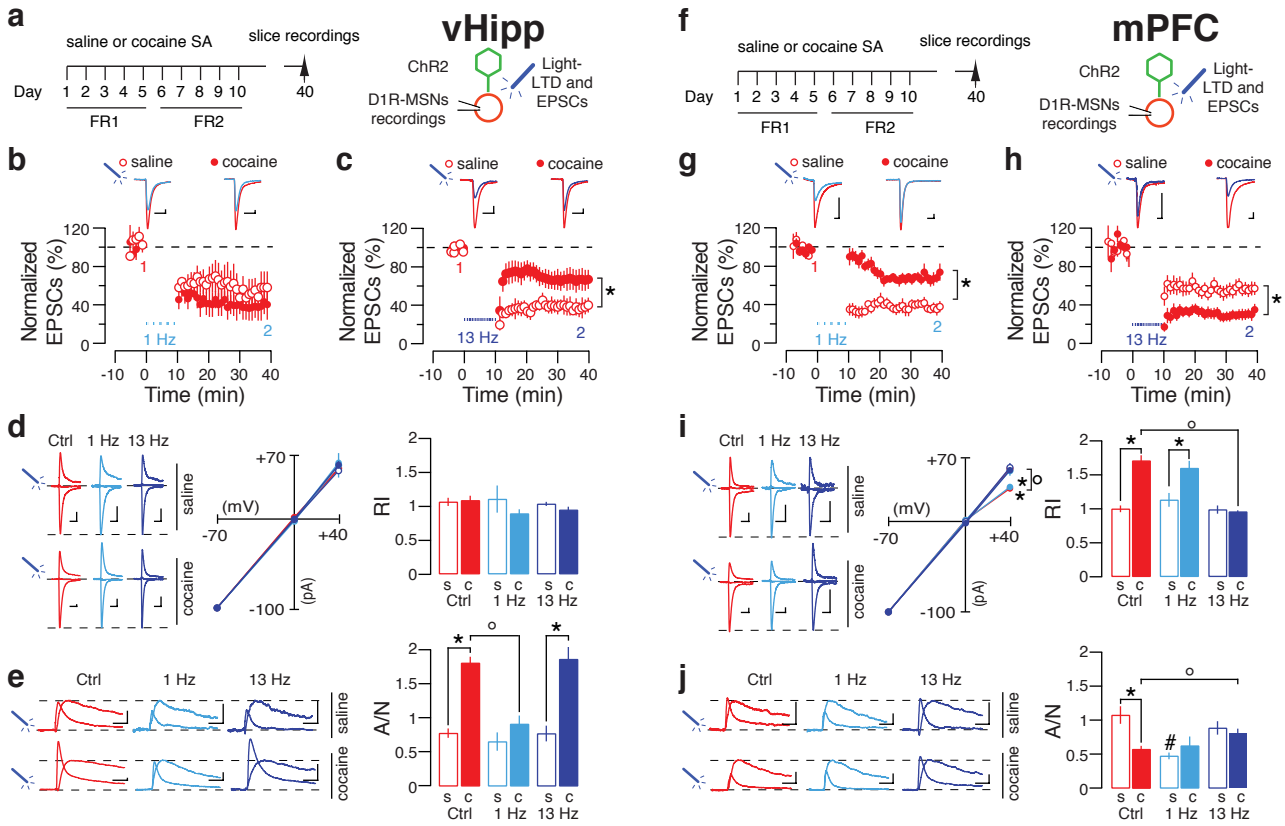
a
saline or cocaine SA
slice recordings
Day
1 2 3 4 5 6 7 8 9 10
40
FR1
FR2
vHipp
ChR2
Light-
LTD and
EPSCs
D1R-MSNs
recordings
f
saline or cocaine SA
slice recordings
Day
1 2 3 4 5 6 7 8 9 10
40
FR1
FR2
mPFC
ChR2
Light-
LTD and
EPSCs
D1R-MSNs
recordings
b
saline
cocaine
Normalized EPSCs (%)
120
80
40
0
1
1 Hz
2
-10 0 10 20 30 40
Time (min)
c
saline
cocaine
Normalized EPSCs (%)
120
80
40
0
1
13 Hz
2
*
-10 0 10 20 30 40
Time (min)
g
saline
cocaine
Normalized EPSCs (%)
120
80
40
0
1
1 Hz
2
*
-10 0 10 20 30 40
Time (min)
h
saline
cocaine
Normalized EPSCs (%)
120
80
40
0
1
13 Hz
2
*
-10 0 10 20 30 40
Time (min)
d
Ctrl 1 Hz 13 Hz
saline
cocaine
+70
(mV)
-70
+40
-100
(pA)
RI
2
1.5
1
0.5
0
s c
Ctrl
s c
1 Hz
s c
13 Hz
i
Ctrl 1 Hz 13 Hz
saline
cocaine
+70
(mV)
-70
+40
-100
(pA)
*
*
o
RI
2
1.5
1
0.5
0
*
*
o
s c
Ctrl
s c
1 Hz
s c
13 Hz
e
Ctrl
1 Hz
13 Hz
saline
cocaine
A/N
2
1.5
1
0.5
0
*
o
*
s c
Ctrl
s c
1 Hz
s c
13 Hz
j
Ctrl
1 Hz
13 Hz
saline
cocaine
A/N
2
1.5
1
0.5
0
*
o
#
s c
Ctrl
s c
1 Hz
s c
13 Hz

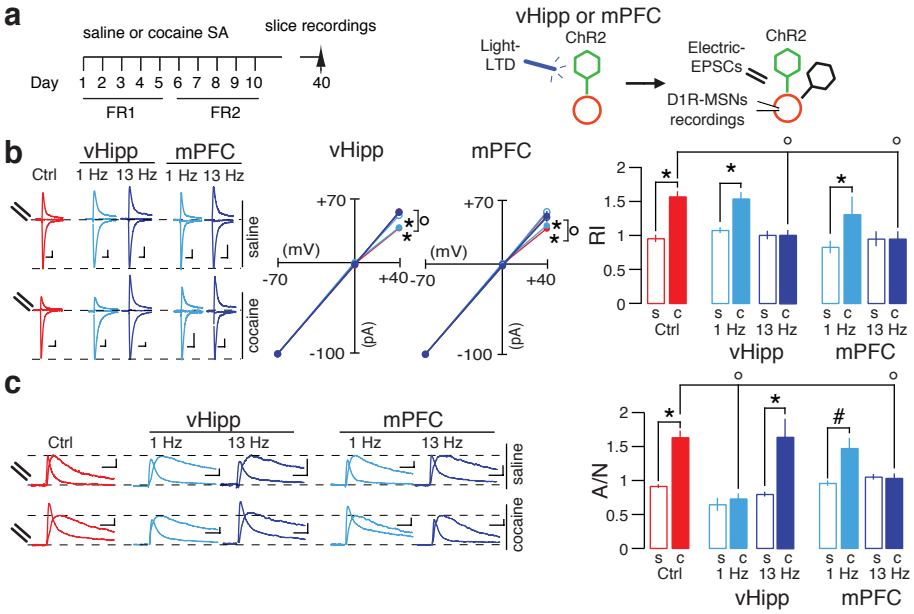
a
saline or cocaine SA
slice recordings
Day
1 2 3 4 5 6 7 8 9 10
40
FR1
FR2
vHipp or mPFC
Light-
LTD
ChR2
Electric-
EPSCs
ChR2
D1R-MSNs
recordings
b
Ctrl
vHipp
mPFC
1 Hz 13 Hz 1 Hz 13 Hz
saline
cocaine
vHipp
mPFC
+70
(mV)
-70
+40
-100
(pA)
RI
2
1.5
1
0.5
0
S C
Ctrl
1 Hz
13 Hz
vHipp
mPFC
c
Ctrl
vHipp
mPFC
1 Hz
13 Hz
saline
cocaine
A/N
#

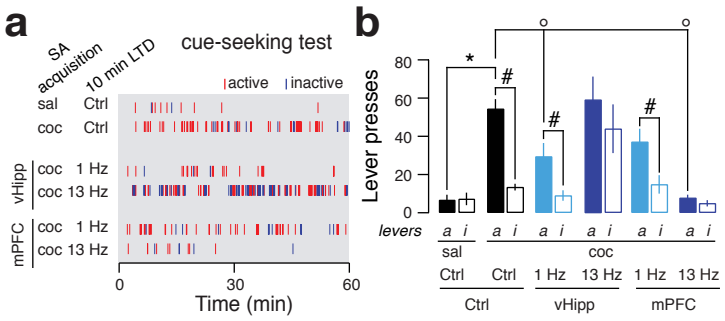
a
SA acquisition
10 min LTD
cue-seeking test
active
inactive
sal Ctrl
coc Ctrl
vHipp
coc 1 Hz
coc 13 Hz
mPFC
coc 1 Hz
coc 13 Hz
0
30
60
Time (min)
b
Lever presses
80
60
40
20
0
levers
a i a i a i a i a i a i
sal
coc
Ctrl Ctrl 1 Hz 13 Hz 1 Hz 13 Hz
Ctrl
vHipp
mPFC
*
#
#
#
°
°